EWI-2 Inhibits Cell-Cell Fusion at the Virological Synapse

Emily E. Whitaker[1,2], Menelaos Symeonides[1,2], Phillip B. Munson[1,3] and Markus Thali[1,2*]

[1]University of Vermont, Department of Microbiology and Molecular Genetics, Burlington, VT, USA
[2]University of Vermont, Graduate Program in Cellular, Molecular, and Biomedical Sciences, Burlington, VT, USA
[3]University of Vermont, Department of Pathology and Laboratory Medicine, Burlington, VT, USA

*** Correspondence:**

Markus Thali
markus.thali@uvm.edu

Keywords: EWI-2, IGSF8, tetraspanin, HIV, cell-cell fusion, virological synapse, T cell

Running title: HIV-1-induced cell-cell fusion is repressed by EWI-2

Word Count: abstract = 254, text = 5,153

Figures: 3

Abstract

Cell-to-cell transfer of virus particles through the virological synapse (VS) is a highly efficient mode of HIV-1 transmission. Formation of the VS, a transient multiform adhesion structure, is mediated through an interaction between the HIV-1 envelope glycoprotein (Env) and the viral receptor CD4 on the surface of infected cell and target cell, respectively. Given that Env, unlike many other viral fusogens, can mediate the merger of membranes at neutral pH, the close encounter of infected and uninfected cells would seem prone to result in cell-cell fusion and thus the formation of syncytia. However, while it is being recognized now that small, T cell-based syncytia are indeed a defining feature of the natural history of HIV-1, the majority of VSs nevertheless resolve without fusion, thus securing continued virus spread. Gag, the main viral structural component, is partially responsible for restraining Env and preventing it from becoming fusogenic before being incorporated into particles. In addition, a few cellular factors, including tetraspanins and ezrin, have also been shown to inhibit Env's activity while this fusogen is still part of the producer cell.

Here, we identify EWI-2, a protein that was previously shown to associate with the tetraspanins CD9 and CD81 and also with ezrin, as a host factor that contributes to the inhibition of Env-mediated cell-cell fusion. Using fluorescence microscopy, flow cytometry, and TZM-bl fusion assays, we show that EWI-2, comparable to tetraspanins, while overall being downregulated upon HIV-1 infection, accumulates at the virological presynapse, thus supporting the fusion-preventing activities of the other viral and cellular components.

1 Introduction

HIV-1 spreads between T cells primarily through two modes of transmission: the release of cell-free virus particles, and cell-to-cell transmission of particles via the virological synapse (VS). Formation of the HIV-1 VS is initiated by the viral envelope glycoprotein (Env) on the surface of productively infected cells binding to its receptor, CD4, on target T cells (1), and is followed by polarization of Gag at the cell-cell contact site (1, 2). Virus particles are then released in high concentrations towards the target cell (3), facilitating efficient infection while also possibly shielding virus particles from some neutralizing antibodies ((4) and reviewed in (5)). Given that Env is fusogenic at neutral pH, it may seem likely at first that VS-mediated contacts would frequently result in cell-cell fusion, thus forming a multinucleated infected cell (syncytium). Indeed, we now know that small, T cell based syncytia arise early in HIV-1 infection (6-9). However, the majority of infected T cells observed in lymphoid tissue are mononucleated, indicating that most HIV-1 VSs ultimately result in complete cell separation and generation of a new, productively infected cell, likely due to tight regulation that acts to prevent excessive syncytium formation (reviewed in (10)).

Multiple independent studies have identified viral and host functions which, together, prevent excessive HIV-1-induced cell-cell fusion at the VS. Firstly, Env is rapidly downregulated from the surface of infected cells in the absence of Gag, thus preventing premature Env-mediated membrane fusion (11, 12). Further, upon Gag multimerization at the plasma membrane, Env is trapped by Gag through Env's cytoplasmic tail and maintained in a non-fusogenic state (13). This trapping by Gag ends only after Env's incorporation into virus particles, when Gag precursor gets cleaved, i.e. upon maturation (14-17). Additionally, several host membrane proteins that accumulate at the producer cell side of the VS, including tetraspanins and ezrin, have been identified as fusion-inhibitory proteins (18-20). Tetraspanins inhibit HIV-1-induced cell-cell fusion at a post-hemifusion stage (19), while ezrin is implicated in F-actin organization and recruitment of tetraspanin CD81 to the VS (20). It remains unclear how and whether these protein functions are coordinated, though based on other cell-cell fusion regulation paradigms (discussed below), additional host proteins are likely required to mediate efficient inhibition of HIV-1-induced fusion by tetraspanins and ezrin.

EWI-F (CD9P-1/FPRP) is an immunoglobulin superfamily (IgSF) member and partner of tetraspanins CD9 and CD81 (21). EWI-F was shown to be a potent inhibitor of cell-cell fusion in myoblasts, where EWI-F knockout resulted in more efficient fusion than CD9/CD81 double knockout (22). However, EWI-F is poorly expressed in T cells (23), the primary host cell type for HIV-1 infection. Another IgSF member and tetraspanin partner protein which is expressed in T cells (21, 23), EWI-2 (IGSF8/PGRL) (24, 25), has been documented to play a role in HCV entry (26, 27) and T cell immunological synapse (IS) formation (28). That latter study by Yáñez-Mó and colleagues also suggested that EWI-2 has a yet undetermined involvement in HIV-1

particle production (28). Furthermore, both EWI-F and EWI-2 interact with ezrin to organize the cytoskeleton in concert with tetraspanins (23). EWI-2 thus lies at the nexus of tetraspanins, ezrin, and the actin cytoskeleton (which can also inhibit cell-cell fusion; (29)) and we therefore sought to test whether EWI-2 contributes to the inhibition of HIV-1-induced cell-cell fusion.

2 Materials and Methods

2.1 Cell Lines and Cell Culture

The following cells were obtained through the NIH AIDS Reagent Program, Division of AIDS, NIAID, NIH: HeLa cells from Dr. Richard Axel (30), TZM-bl cells from Dr. John C. Kappes, Dr. Xiaoyun Wu, and Tranzyme Inc. (31-35) and CEM-SS cells from Dr. Peter L. Nara (30, 36, 37).

HEK 293T, HeLa, and TZM-bl cells were maintained in Dulbecco's Modification of Eagle's Medium (DMEM) (Corning, Corning, NY, Cat. #10-017-CV) containing 10% fetal bovine serum (FBS; Corning, Cat. #35-010-CV) and antibiotics (100 units/mL penicillin and 100 µg/mL streptomycin; Invitrogen). CEM2n, a kind gift from R. Harris (38), and CEM-SS cells were maintained in RPMI 1640 medium (Corning, Cat. #10-104-CV) supplemented with 10% FBS and antibiotics.

Human primary blood mononuclear cells (PBMCs) were isolated as buffy coats from whole blood of healthy donors by Ficoll density centrifugation. $CD4^+$ T cells were enriched from PBMCs by negative selection using the MACS $CD4^+$ T Cell Isolation Kit (Miltenyi Biotec, Auburn, CA, Cat. #130-096-533) according to manufacturer's instructions. Primary $CD4^+$ T cells were activated in RPMI containing 10% FBS, 50 units/mL IL-2, antibiotics, and 5 µg/mL phytohemagglutinin. After 48 h of activation, cells were washed and subsequently maintained and expanded in the same medium but without phytohemagglutinin. Cells were used for infections at 4 to 7 days post isolation.

2.2 Antibodies

Mouse monoclonal antibody (mAb) to EWI-2 (8A12) was a kind gift from Dr. Eric Rubinstein (21). Mouse mAb to HIV-1 p24 (AG3.0) was obtained through the NIH AIDS Reagent Program, Division of AIDS, NIAID, NIH, from Dr. Jonathan Allan (39). Rabbit antiserum to HIV-1 p6 was a kind gift from David E. Ott. Rabbit polyclonal antibody (pAb) to HIV-1 p24 was obtained from Advanced Biotechnologies (Cat. #13-203-000). Secondary antibodies were as follows: Alexa Fluor 488-conjugated donkey pAb to mouse IgG (Invitrogen, Cat. #A21202), Alexa Fluor 488-conjugated donkey pAb to rabbit IgG (Invitrogen Cat. # A21206), Alexa Fluor 594-conjugated donkey pAb to mouse IgG (Invitrogen Cat. #R37115), Alexa Fluor 594-conjugated donkey pAb to rabbit IgG (Invitrogen Cat. # A21207), Alexa Fluor 647-conjugated donkey pAb to mouse IgG (Invitrogen Cat. #A31571), and Alexa Fluor 647-conjugated goat pAb to mouse IgG (Invitrogen Cat. #A21235). Zenon labeling of primary antibodies with either Alexa Fluor 488 or Alexa Fluor 594 was carried out using Zenon Labeling Kits according to the manufacturer's instructions (Molecular Probes, Eugene, OR, Cat. #Z25002 and #Z25007).

2.3 Plasmids and Virus Strains

pcDNA3, pCDNA3.1, and pCMV SPORT6 (Invitrogen) were vectors for EWI-2, CD81, and L6 overexpression, respectively. Proviral plasmids pNL4-3 or pNL4-3 ΔEnv (KFS) were a kind gift from Dr. Eric Freed (National Cancer Institute, Frederick, MD, USA) (40). NL4-3-derived fluorescent protein-tagged proviral plasmids pNL-sfGI and pNL-sfGI ΔEnv (9) were kind gifts from Dr. Benjamin Chen (Mount Sinai School of Medicine, New York, NY). Vesicular stomatitis virus glycoprotein (VSV-G) was used to pseudotype viral stocks produced in HEK 293T cells.

2.4 Virus Stocks and Infections

VSV-G-pseudotyped virus stocks of NL4-3, NL4-3 ΔEnv, NL-sfGI, and NL-sfGI ΔEnv were produced in HEK 293T cells transfected with the proviral plasmid and pVSV-G (at 17:3 ratio) using calcium phosphate precipitation. Supernatants were harvested 2 days after transfection, cleared by centrifugation at 2000 rcf for 10 min, filtered, and stored at -80˚C.

To infect CEM2n cells by spinoculation, two million cells were incubated with RPMI/10% FBS containing 90 µL of virus stock (resulting in ~3% of the cells being infected) or medium alone (for uninfected controls), for 20 min at 37 ˚C, followed by centrifugation at 1200 rcf for 2 h at 37˚C. Cell pellets were allowed to recover at 37 ˚C for 15 min, centrifuged at 300 rcf for 2 min, and resuspended in fresh RPMI/10% FBS. Cells were incubated at 37 ˚C, the medium was refreshed 2 days post infection, and the cells were used 1 day later for all subsequent experiments.

To infect primary $CD4^+$ T cells, 1 or 2 million cells were incubated in RPMI/10% FBS/IL-2 containing 200 or 400 µL of virus, respecitively, and spinoculated as described above. Cells were resuspended in fresh RPMI/10% FBS/PS/IL-2 and incubated at 37 ˚C/5% CO_2. Cells were used 2 days post infection for all subsequent experiments.

To infect CEM-SS cells by shaking, one or two million cells suspended in CO_2-independent medium (Gibco) supplemented with 10% FBS were mixed with VSV-G-pseudotyped virus stocks and shaken at 220 rpm for 2 h at 37 ˚C. Cells were then washed and plated in fresh RPMI/10% FBS, and used for experiments as described.

2.5 Quantification of EWI-2 accumulation at the VS

CEM-SS and primary $CD4^+$ T cells were infected with VSV-G-pseudotyped NL4-3 or NL4-3 ΔEnv virus by shaking or spinoculation, respectively. Two days post infection, uninfected CEM-

SS target cells were labeled with CMAC (Invitrogen) according to manufacturer's instructions, mixed with infected cells at a 1:1 or 1:2 ratio (infected:target), seeded onto the microwell of a 35 mm glass-bottom dish (MatTek Corporation, Ashland, MA, Cat. #P35G-1.5-14-C) coated with poly-L-Lysine (Sigma), and incubated at 37˚ C for 3 to 4.5 h. For primary cells, uninfected cells were mixed with infected cells at a 1:1 or 1:2 ratio (infected:target), seeded onto 8-well glass-bottom plates (CellVis, Mountain View, CA, Cat. #C8-1.5H-N) coated with 1:10 poly-L-Lysine in ddH_2O, and incubated for 2 h at 37˚ C. CEM-SS and primary cells were then chilled on ice and surface-labeled with 1:200 mouse anti-EWI-2 mAb (8A12) in RPMI/10% FBS for 30 or 45 min, respectively, at 4 ˚C. Surface-labeled cells were fixed with 4% PFA in PBS at room temperature for 10 min. CEM-SS cells were blocked and permeabilized overnight with 1% BSA and 0.2% Triton X-100 in PBS (block/perm). Primary cells were blocked and permeabilized with PBS containing 1% BSA and 100 µg/mL digitonin for 10 min. All CEM-SS conditions were labeled with Alexa Fluor 647-conjugated anti-mouse secondary pAb in block/perm buffer at 1:500 dilution. NL4-3 and NL4-3 ΔEnv-infected conditions were subsequently stained with Alexa Fluor 594 Zenon-labeled anti-p24 AG3.0 mAb, and fixed again with 4% PFA in PBS. Primary cells were labeled with a mixture of rabbit anti-p24 and anti-p6 antibodies, each at 1:1000 dilution, in PBS with 1% BSA for 1 h. Subsequently, primary cells were labeled with Alexa Fluor 647, 594, or 488-conjugated anti-mouse or anti-rabbit secondary pAb as indicated. All cells were kept in PBS for imaging.

To visualize only producer cell-associated EWI-2 at the VS, 400,000 target TZM-bl cells (which express undetectable levels of EWI-2) were seeded onto the entire surface of a 35 mm glass-bottom dish one day prior to co-culture. The next day, 250,000 CEM-SS cells (infected 3 days prior as described above) were added to the glass microwell of the dish. Five hours later, the cells were surface-labeled with 1:200 mouse anti-EWI-2 mAb (8A12; Zenon-labeled with Alexa Fluor 594) in RPMI/10% FBS on ice for 30 min. Cells were subsequently fixed with 4% PFA in PBS and permeabilized with block/perm for 10 min. Cells were kept in PBS for imaging.

Images were acquired on a DeltaVision epifluorescence microscope (GE/Applied Precision, Issaquah, WA, USA) with an Olympus IX-70 base using an Olympus 60× PlanApo 1.42 NA objective and equipped with a CoolSNAP HQ CCD camera (Photometrics). Images were imported into Fiji for analysis following deconvolution and cropping using Softworx software. The VS was identified using the Gag channel and the level of EWI-2 accumulation was determined by measuring its signal intensity at the VS. For ΔEnv controls, cell-cell contacts were identified using the brightfield channel and treated analogous to a VS. To determine the level of enrichment at the VS (or cell-cell contact), EWI-2 signal intensity at that site was divided by the average EWI-2 signal at several non-contact sites on the same cell.

2.6 Determining surface levels of EWI-2 by microscopy

To compare EWI-2 surface expression between infected and uninfected cells, CEM2n cells were infected with VSV-G-pseudotyped NL-sfGI as described above. Three days post infection, 3×10^5 infected cells were plated onto each well of 8-well glass-bottom plates coated with 1:10 poly-L-Lysine in ddH_2O. Two additional wells were used for uninfected controls. After 2 h of incubation at 37 ˚C, the medium was replaced with ice cold RPMI/10% FBS containing mouse anti-EWI-2 mAb (8A12) at 1:200 dilution for surface labeling, and incubated for 45 min at 4 ˚C. Following the primary antibody incubation, cells were washed with RPMI/10% FBS and fixed with 4% PFA in PBS for 10 min at 4 ˚C, blocked and permeabilized with PBS containing 1% BSA and 100 µg/mL digitonin for 10 min, and incubated with the indicated secondary antibody in PBS containing 1% BSA for 45 min at room temperature. Cells were washed with PBS containing 1% BSA and imaged in PBS. At least 50 fields containing infected cells were selected for each biological replicate and imaged, deconvolved and cropped using the DeltaVision microscope and Softworx software described above. Images were imported into Fiji for analysis. Background fluorescence was determined using uninfected controls only incubated with the secondary antibody and not the primary, and subtracted from all images by adjusting the minimum brightness of each channel. Threshold masks were applied to all images to aid in the visualization of channels containing GFP and Alexa Fluor 594 or 647-associated signal for infected cells and EWI-2 surface staining, respectively. Figure 2A is a representative image, without threshold masks, from 3 independent experiments with 2 replicates each.

To quantify surface levels of EWI-2 on HIV-1-infected primary $CD4^+$ T cells by microscopy, cells at two days post infection were plated, surface-stained for EWI-2, and imaged as described above. After deconvolution in Softworx, Fiji was used to manually select the cell surface at the midline of each cell and the mean intensity of EWI-2-associated signal was quantified and subsequently subtracted by the mean intensity of an area that did not contain cells. Only cells not contacting other cells were used for quantification. The virus-associated fluorescent reporter channel was used to segregate measurements into uninfected and infected. The data shown in Figure 2D are pooled from 2 independent biological replicates, each consisting of 2 technical replicates, all of which were sampled randomly until a total of 100 infected cells were quantified.

2.7 Determining surface EWI-2 signal on infected cells by flow cytometry

CEM2n cells infected as described above were harvested after three days and incubated in cold PBS with 5 mM EDTA for 15 min (3.0×10^5 cells/tube). Cells were pelleted at 400 rcf for 7 min at 4 °C and resuspended in cold RMPI/10% FBS containing mouse anti-EWI-2 mAb (8A12) at 1:200 dilution. After a 45 min incubation at 4 °C, cells were washed with cold RPMI/10% FBS and resuspended in ice cold PBS with 5 mM EDTA. To fix, an equal volume of PBS with 8% PFA was added and samples were incubated on ice for 10 min. Cells were washed and stained

with Alexa Fluor 594-conjugated secondary antibody at 1:500 in PBS with 1% BSA for 45 min at room temperature, before being washed, resuspended in PBS, and analyzed using a BD LSRII flow cytometer. Data were analyzed using FlowJo V10 (Becton, Dickinson & Company, Franklin Lakes, NJ). Samples were gated for infected and uninfected populations by GFP expression. EWI-2 wild-type (WT) and EWI-2 low gates were set based in part on controls lacking primary antibody, and in part by adjusting the gates to reflect the number of uninfected EWI-2 WT cells as measured by microscopy. The data shown are the collection of 3 independent biological replicates, each consisting of 2 technical replicates.

2.8 HIV-1-induced cell-cell fusion assay

50,000 HeLa cells were plated in each well of a 24-well plate and, the next day, transfected in duplicate or triplicate with 0.1 µg of either pNL-sfGI or pNL-sfGI ΔEnv along with 0.5 or 0.625 µg total expression vector carrying the protein of interest (L6, CD81, or EWI-2) using FuGene6 transfection reagent at a ratio of 3:1 (Fugene6:DNA) according to manufacturer's instructions (Promega, Madison, WI, Cat. #E2691). For dose response assays, 0.125, 0.25, or 0.5 µg of the protein expression plasmid of interest was co-transfected with L6 expression plasmid to maintain 0.5 µg of total protein expression plasmid in each condition. For EWI-2 and CD81 co-transfections, 0.5 µg of EWI-2 was co-transfected with 0.125 µg of CD81, while conditions where only either EWI-2 or CD81 was expressed were brought up to 0.625 µg of total overexpression plasmid using L6 as described above. Each transfection condition was performed in duplicate or triplicate within each biological replicate. 24 h post-transfection, producer HeLa cells were co-cultured with 10^6 TZM-bl target cells (which upon producer-target cell fusion, express firefly luciferase under control of the HIV-1 LTR) per well for 3 h before unattached target cells were washed off and the medium was refreshed. 14-18 h later, cells were lysed for at least 30 min on ice using 1% Triton X-100, 2mM EDTA, 50 mM Tris-HCl, 200 mM NaCl, with 1% protease inhibitor cocktail (Millipore Sigma, Darmstadt, Germany, Cat. #P8340). Lysates were precleared by centrifugation at 20,000 rcf for 5 min at 4 °C and stored at -80°C until use for luciferase activity assays.

Each lysate was incubated with an equal volume of firefly luciferase reagent (Promega, Cat. #E1500) for 1 min in a 96-well white-walled plate (ThermoFisher Scientific, Waltham, MA, Cat. #7571) before collecting luminescence signal intensity on a microplate reader (BioTek Synergy 2). Background luminescence was determined using a lysis buffer blank and subtracted from all experimental samples. Luminescence intensity was used as a quantitave measurement of relative HeLa-TZM syncytium formation against the non-fusogenic, ΔEnv control. The data shown are the collection of 5 and 2 independent biological replicates, for the dose response and co-transfection assays, respectively.

2.9 Statistical Analysis

All statistical analyses were carried out in GraphPad Prism 7 using a two-tailed non-parametric Mann-Whitney U test (Figure 1, Figure 2D) or student's paired *t*-test (Figures 2B-C).

3. Results

3.1 EWI-2 localizes at the virological presynapse in HIV-1-infected CEM-SS cells

Because EWI-2 is known to associate with ezrin and CD81 (21, 23), two cellular factors that we have previously found to accumulate at the producer cell side of the VS (20, 41), we first sought to determine whether this protein also localizes to the virological presynapse. CEM-SS cells were infected with (VSV-G-pseudotyped) NL4-3 WT, or NL4-3 ΔEnv (virus that does not express Env) and mixed with target CEM-SS cells (labeled with a cytoplasmic dye). Upon imaging with a 60× objective, the VS was identified as clusters of immunolabeled Gag present at producer-target contact sites. Similarly to ezrin and CD81 (20, 41), EWI-2 was observed to co-accumulate with Gag at the VS in an Env-dependent manner (Figure 1A, left and inset). EWI-2 signal intensity was ~4-fold enhanced at the VS in CEM-SS cells infected with NL4-3 WT, while no EWI-2 enrichment was seen at cell-cell contacts in cells infected with NL4-3 ΔEnv (Figure 1A). EWI-2 signal intensity was also enhanced ~2-fold at the VS in NL4-3 WT-infected primary $CD4^+$ T cells compared to non-VS contact sites (ΔEnv) (Figure 1B). To determine whether EWI-2 enrichment at the VS takes place within the infected cell (rather than the apposed uninfected target cell), i.e. at the presynapse, HIV-1-infected CEM-SS cells were co-cultured with uninfected target TZM-bl cells (which do not have detectable EWI-2 on their surface) and imaged as described above. EWI-2 enrichment was observed at the VS as before (Figure 1A, bottom half), demonstrating that the observed EWI-2 accumulation in CEM-SS-CEM-SS co-cultures takes place at least partially within the producer cell. Together, these results document that EWI-2 is recruited to the virological presynapse during HIV-1 cell-to-cell transmission.

3.2 Overall surface levels of EWI-2 are decreased in HIV-1-infected cells

Despite their enrichment at the virological presynapse, the EWI-2 partner proteins CD81 and ezrin are overall downregulated in HIV-1-infected cells (20, 41). We therefore tested whether surface levels of EWI-2 are similarly decreased in lymphocytes infected with HIV-1 NL-sfGI, a strain in which superfolder GFP (sfGFP) replaces the Nef gene and Nef expression is restored using an IRES (9). We chose to utilize a GFP reporter virus rather than immunolabeling Gag after fixation because Gag-negative cells still in the early phase of infection can still exhibit host protein downregulation due to early Nef expression (unpublished observation and reviewed in (42)). We also observed that surface levels of EWI-2 in uninfected CEM-SS cells were considerably higher than in other T lymphocytes, including primary $CD4^+$ T cells, and that EWI-2 levels in the near-diploid CEM-derived cell line CEM2n (38) were most similar to primary cells (unpublished observations). We therefore here present data from CEM2n and primary cells only, though we found similar effects in other lymphocytes including CEM-SS cells (unpublished observations).

HIV-1-infected CEM2n cells adhered to glass-bottom dishes were surface-labeled with EWI-2 primary antibody on ice, and fixed before incubation with Alexa Fluor 594-conjugated secondary antibody. Uninfected and HIV-1-infected cells were imaged with a 60× objective and the resulting images were deconvolved. Threshold masks (not shown) were applied using Fiji to identify infected cells (i.e. GFP-expressing) and levels of EWI-2 that were clearly discernible above background secondary antibody binding were determined using appropriate controls. The presence of EWI-2 on each cell was scored as WT or low based on the expression patterns of uninfected controls (representative image shown in Figure 2A). Scoring showed that, on average across three independent biological replicates, ~65% of uninfected cells had WT surface levels of EWI-2, while only ~25% of infected cells had WT EWI-2 surface levels (Figure 2B).

We also sought to quantify the frequency of cells with WT and low EWI-2 surface expression by flow cytometry as a means of high-throughput analysis that would include EWI-2 regulation at all stages of HIV-1 infection. HIV-1 NL-sfGI-infected CEM2n cells, surface-labeled for EWI-2 and analyzed by flow cytometry, were gated for WT or low levels of EWI-2 (analogous to the thresholding method described above). These data showed that significantly fewer infected cells (identified as GFP^+) had WT levels of EWI-2 surface expression than uninfected cells (identified as GFP^-) in the same culture (Figure 2C, left). Additionally, the mean fluorescence intensity of EWI-2-associated signal was lower within the total population of infected cells compared to that of the uninfected cells (Figure 2C, right).

Similar downregulation of surface EWI-2 was also observed in HIV-1-infected primary $CD4^+$ T cells (Fig. 2D). In this case, the relatively low baseline levels and mostly punctate appearance of surface EWI-2 in primary cells precluded imaging threshold-based quantification as above. Instead, data were analyzed by measuring the mean intensity of EWI-2-associated signal at manually-selected regions representing the cell surface.

Overall, both the quantitative imaging (Figures 2B and 2D) and the flow cytometric analyses (Fig. 2C) showed that EWI-2 surface levels, similar to those of CD81 and ezrin, are decreased in HIV-1-infected T lymphocytes.

3.3 EWI-2 overexpression lowers the frequency of HIV-1-induced syncytium formation

Likely through their accumulation at the producer cell side of the VS, the EWI-2 partner proteins CD81 and ezrin repress fusion of infected and uninfected cells, i.e. syncytium formation (18-20). Given that EWI-2 also accumulates at the VS (Figure 1), we sought to test whether it also contributes to the inhibition of HIV-1-induced syncytium formation. Attempts to determine whether knocking down EWI-2 expression in lymphocytes enhances HIV-1-induced syncytium formation were unsuccessful at this time due to technical difficulties. In parallel, and as we have done previously to examine the fusion-inhibitory capacity of tetraspanins (18, 19), we chose to

test whether EWI-2 may act as an inhibitor of HIV-1-induced syncytium formation by overexpressing EWI-2 in HeLa cells. The results of those experiments are presented here.

NL-sfGI-producing HeLa cells overexpressing either EWI-2, CD81, or L6 (a tetraspanin-like surface protein that does not repress HIV-1-induced cell-cell fusion; (19, 43)) were co-cultured with uninfected target TZM-bl cells. As a negative control for HIV-1-induced cell-cell fusion, Env-deleted NL-sfGI-expressing HeLa cells were also co-cultured with target TZM-bl cells. HIV-1-induced HeLa-TZM-bl syncytia express firefly luciferase under control of the HIV-1 LTR (18). After 3 h of co-culture (and another 14-18 h to allow for reporter expression), cells were lysed, the lysates were incubated with luciferase reagent, and luminescence was measured using a microplate reader. Overexpression of increasing amounts of EWI-2 (0.125, 0.25, or 0.5 µg of plasmid) in NL-sfGI-producing cells resulted in robust and dose-dependent decrease of cell-cell fusion (at 0.25 and 0.5 µg of input plasmid), though repression was not as extensive as that observed upon CD81 overexpression (Figure 3A).

3.4 No evidence for synergistic cell-cell fusion repression by EWI-2 and CD81

EWI-2 is a close relative of another tetraspanin partner protein, EWI-F (CD9P-1), which acts alongside the tetraspanins CD9 and CD81 to inhibit myoblast fusion (22). Given that, in that study, EWI-F ablation resulted in the hyperfusion phenotype faster than CD81/CD9 silencing, it was speculated that EWI-F may regulate fusion inhibition mediated by the two tetraspanins, though this was not yet tested. Here, we thus sought to analyze if EWI-2 can cooperate with CD81 to repress HIV-1-induced syncytium formation, possibly even in a synergistic manner.

The results of the dose-response curves in Figure 3A were used to determine the amount of either the CD81 or the EWI-2 overexpression plasmid that, when co-transfected with pNL-sfGI, resulted in a moderate (~30%) inhibition of syncytium formation (0.125 and 0.5 µg, respectively). Should these proteins be able to synergistically repress cell-cell fusion, one would expect that co-transfecting those amounts of each plasmid, alongside HIV-1 pNL-sfGI, should result in an overall inhibition of virus-induced syncytium formation of greater than 60%. As shown, however, in Figure 3B, the combination of the two fusion repressors resulted in an inhibition of syncytium formation of only ~50%. Thus, at least under the experimental conditions used here, EWI-2 and CD81 do not act synergistically.

4 Discussion

Transient alignment of infected (producer) and uninfected (target) cells allows for very efficient transmission of virus particles. However, because of the presence of viral Env and viral receptors at the surface of producer and target cell, respectively, rather than separating after particle transfer, these cells could also easily fuse with each other, thus forming a syncytium. Various viral and cellular factors have been identified which, together, reduce the likelihood of such syncytium formation, and this study now allows us to add EWI-2 to the list of host factors that repress HIV-1 Env-mediated cell-cell fusion.

Our investigations were prompted partially by two recent reports. In one of those studies, Rubinstein and colleagues documented a role for EWI-F, a close relative of EWI-2, in myoblast fusion regulation (22). EWI-F was shown to act as fusion repressor in cooperation with the tetraspanins CD9 and CD81. With the other study, Yáñez-Mó and colleagues (28) showed the presence of EWI-2 at sites of contact between uninfected T cells and T cells stably expressing HIV-1 Env. In separate experiments, HIV-1-infected EWI-2 knockdown cells were also shown to have somewhat increased virus production and the authors mentioned (as data not shown) that this was accompanied by augmented syncytium formation, indicating that EWI-2 could be involved in the regulation of HIV-1-induced membrane fusion. The study did not, however, address the question of whether the reported increase in syncytium formation was (potentially) caused by the action of EWI-2 in producer or target cells, though the authors speculated that EWI-2, together with α-actinin, might be active in target cells, there possibly contributing to α-actinin's actin bundling activity, thus ultimately inhibiting virus entry/fusion. They explicitly stated, however, that they cannot exclude an involvement of EWI-2 in "subsequent steps of the viral life cycle".

Our study now reveals that this is indeed the case: during the late phase of the HIV-1 replication cycle, EWI-2 accumulates on the producer cell side of the VS (Figure 1), and, the results of experiments shown in Figure 3 reveal that such accumulation at the virological presynapse correlates with decreased syncytium formation. Such EWI-2 accumulation and fusion-inhibiting function at the producer cell side of the VS parallels the activities of tetraspanins that also accumulate at the presynapse (41, 44, 45), recruited by viral Gag (46). Also paralleling what we observed for tetraspanins (18), we found that fusion with uninfected target cells was inhibited by EWI-2 in a dose-dependent manner (Figure 3A). While, at first sight, CD81 appears to be a more potent inhibitor of cell-cell fusion than EWI-2, at this point we cannot determine whether this is a consequence of other factors, e.g. the levels of EWI-2 or CD81 achieved upon transfection, or whether the absence of endogenous EWI-2 in HeLa producer cells means that overexpressed EWI-2 is quickly downregulated (unlike CD81, which is highly expressed at baseline, thus likely saturating the ability of the virus to downregulate it already before overexpression). Further investigations are required to appropriately compare the contribution of each fusion inhibitor.

Given that EWI-2 associates with the tetraspanins CD9 and CD81 (24, 25, 47), it would have seemed plausible that EWI-2 and CD81 act synergistically to prevent syncytium formation. As shown in Figure 3B, however, we found that the level of fusion inhibition upon EWI-2 and CD81 co-transfection was lower than the sum of the inhibition by each protein individually, i.e. their fusion inhibitory functions do not even seem to be additive as one would have expected if the two proteins act separately. A possible explanation for the observed result would be that EWI-2 desensitizes cells to fusion inhibition by overexpressed CD81, again possibly because of the high baseline levels of CD81, so that any additional CD81 protein might be sequestered by EWI-2 rather than allowed to overaccumulate at VSs (48). Alternatively, synergistic fusion inhibition might require a particular ratio of EWI-2 to CD81 during a narrow time window (when Env triggers cell-cell fusion), something that might not be achieved in a simple co-transfection setting.

Interestingly, and paralleling our findings about tetraspanin expression in HIV-1-infected cells (41, 49), while EWI-2 accumulates at the virological presynapse, overall this protein is downregulated in infected cells (Figure 2). Importantly, and again similar to our tetraspanin data which were confirmed by an independent study (50), in two recent proteomics screens (51, 52) EWI-2 was found to be one of the host proteins whose expression is diminished in HIV-1-infected T cells. The combination of these two features, i.e. enrichment during one step of the viral replication cycle (assembly and transmission at the VS) and overall downregulation specifically in infected cells, strongly suggests that a particular host factor plays an important role in virus replication, and given the fusion-preventing functions documented in this study, we certainly think this holds true for EWI-2.

Finally, EWI-2's contribution to repressing the formation of HIV-1-induced syncytia may be relevant mostly because this allows for continued spread of the virus since the number of infected cells duplicates each time when producer and target cells separate after virus transmission. Additionally, we and others have recently shown that lowering Env's fusion activity and thus its syncytium forming ability also allows HIV-1 to overcome a restriction factor (APOBEC3G; (53)), and even antiviral drugs (Van Duyne and Freed, pers. communication). Importantly, the action of this protein along with others could also help the virus, or, rather, HIV-1-infected cells, to evade the host immune response. For instance, simply because syncytia are larger and thus more "visible" than individual infected cells, they may be more prone to be attacked by innate immune cells. In addition, unpublished studies in our lab suggest that these entities have a different surface profile of immune regulatory proteins compared to mononucleated infected cells, similar to how e.g. measles virus-induced syncytia show an upregulation of ligands of activating natural killer cell receptors (54). Thus, fusion-repressing host factors such as EWI-2, whose syncytium-inhibiting function we identify in this report, besides supporting efficient virus spread, probably also help HIV-1 escape attacks by the human immune system.

5 Acknowledgments

The flow cytometry data we presented were obtained at the Harry Hood Bassett Flow Cytometry and Cell Sorting Facility, Larner College of Medicine, University of Vermont. The imaging shown in Figure 1A was performed at the Imaging/Physiology Core Facility, Neuroscience Center of Biomedical Research Excellence, Larner College of Medicine, University of Vermont.

6 Author Contributions Statement

EW, MS, and MT conceived and designed the experiments. EW, MS, and PM performed the experiments and analyzed the results. EW and MS prepared the figures. EW, MS, and MT wrote and edited the manuscript.

7 Conflict of Interest Statement

The authors declare no competing commercial or financial interests.

8 Funding

The work was supported by the National Institutes of Health (R01-GM117839 to MT, P30-RR032135 and P30-GM103498 for the Neuroscience COBRE Imaging Facility). The contents are solely the responsibility of the authors and do not necessarily represent the official views of NIH.

9 References

1. Jolly C, Kashefi K, Hollinshead M, Sattentau QJ. HIV-1 cell to cell transfer across an Env-induced, actin-dependent synapse. *J Exp Med* (2004) 199(2):283-93. doi: 10.1084/jem.20030648.
2. Hubner W, McNerney GP, Chen P, Dale BM, Gordon RE, Chuang FY, et al. Quantitative 3D video microscopy of HIV transfer across T cell virological synapses. *Science* (2009) 323(5922):1743-7. doi: 10.1126/science.1167525.
3. Ladinsky MS, Kieffer C, Olson G, Deruaz M, Vrbanac V, Tager AM, et al. Electron tomography of HIV-1 infection in gut-associated lymphoid tissue. *PLoS Pathog* (2014) 10(1):e1003899. doi: 10.1371/journal.ppat.1003899.
4. Reh L, Magnus C, Schanz M, Weber J, Uhr T, Rusert P, et al. Capacity of Broadly Neutralizing Antibodies to Inhibit HIV-1 Cell-Cell Transmission Is Strain- and Epitope-Dependent. *PLoS Pathog* (2015) 11(7):e1004966. doi: 10.1371/journal.ppat.1004966.
5. Bracq L, Xie M, Benichou S, Bouchet J. Mechanisms for Cell-to-Cell Transmission of HIV-1. *Front Immunol* (2018) 9:260. doi: 10.3389/fimmu.2018.00260.
6. Orenstein JM. In vivo cytolysis and fusion of human immunodeficiency virus type 1-infected lymphocytes in lymphoid tissue. *J Infect Dis* (2000) 182(1):338-42. doi: 10.1086/315640.
7. Murooka TT, Deruaz M, Marangoni F, Vrbanac VD, Seung E, von Andrian UH, et al. HIV-infected T cells are migratory vehicles for viral dissemination. *Nature* (2012) 490(7419):283-7. doi: 10.1038/nature11398.
8. Symeonides M, Murooka TT, Bellfy LN, Roy NH, Mempel TR, Thali M. HIV-1-Induced Small T Cell Syncytia Can Transfer Virus Particles to Target Cells through Transient Contacts. *Viruses* (2015) 7(12):6590-603. doi: 10.3390/v7122959.
9. Law KM, Komarova NL, Yewdall AW, Lee RK, Herrera OL, Wodarz D, et al. In Vivo HIV-1 Cell-to-Cell Transmission Promotes Multicopy Micro-compartmentalized Infection. *Cell Rep* (2016) 15(12):2771-83. doi: 10.1016/j.celrep.2016.05.059.
10. Compton AA, Schwartz O. They Might Be Giants: Does Syncytium Formation Sink or Spread HIV Infection? *PLoS Pathog* (2017) 13(2):e1006099. doi: 10.1371/journal.ppat.1006099.
11. Rowell JF, Stanhope PE, Siliciano RF. Endocytosis of endogenously synthesized HIV-1 envelope protein. Mechanism and role in processing for association with class II MHC. *J Immunol* (1995) 155(1):473-88.
12. Egan MA, Carruth LM, Rowell JF, Yu X, Siliciano RF. Human immunodeficiency virus type 1 envelope protein endocytosis mediated by a highly conserved intrinsic internalization signal in the cytoplasmic domain of gp41 is suppressed in the presence of the Pr55gag precursor protein. *J Virol* (1996) 70(10):6547-56.
13. Roy NH, Chan J, Lambele M, Thali M. Clustering and mobility of HIV-1 Env at viral assembly sites predict its propensity to induce cell-cell fusion. *J Virol* (2013) 87(13):7516-25. doi: 10.1128/jvi.00790-13.
14. Murakami T, Ablan S, Freed EO, Tanaka Y. Regulation of human immunodeficiency virus type 1 Env-mediated membrane fusion by viral protease activity. *J Virol* (2004) 78(2):1026-31.
15. Wyma DJ, Jiang J, Shi J, Zhou J, Lineberger JE, Miller MD, et al. Coupling of human immunodeficiency virus type 1 fusion to virion maturation: a novel role of the gp41 cytoplasmic tail. *J Virol* (2004) 78(7):3429-35.

16. Jiang J, Aiken C. Maturation-dependent human immunodeficiency virus type 1 particle fusion requires a carboxyl-terminal region of the gp41 cytoplasmic tail. *J Virol* (2007) 81(18):9999-10008. doi: 10.1128/jvi.00592-07.
17. Chojnacki J, Staudt T, Glass B, Bingen P, Engelhardt J, Anders M, et al. Maturation-dependent HIV-1 surface protein redistribution revealed by fluorescence nanoscopy. *Science* (2012) 338(6106):524-8. doi: 10.1126/science.1226359.
18. Weng J, Krementsov DN, Khurana S, Roy NH, Thali M. Formation of syncytia is repressed by tetraspanins in human immunodeficiency virus type 1-producing cells. *J Virol* (2009) 83(15):7467-74. doi: 10.1128/jvi.00163-09.
19. Symeonides M, Lambele M, Roy NH, Thali M. Evidence showing that tetraspanins inhibit HIV-1-induced cell-cell fusion at a post-hemifusion stage. *Viruses* (2014) 6(3):1078-90. doi: 10.3390/v6031078.
20. Roy NH, Lambele M, Chan J, Symeonides M, Thali M. Ezrin is a component of the HIV-1 virological presynapse and contributes to the inhibition of cell-cell fusion. *J Virol* (2014) 88(13):7645-58. doi: 10.1128/jvi.00550-14.
21. Charrin S, Le Naour F, Oualid M, Billard M, Faure G, Hanash SM, et al. The major CD9 and CD81 molecular partner. Identification and characterization of the complexes. *J Biol Chem* (2001) 276(17):14329-37. doi: 10.1074/jbc.M011297200.
22. Charrin S, Latil M, Soave S, Polesskaya A, Chretien F, Boucheix C, et al. Normal muscle regeneration requires tight control of muscle cell fusion by tetraspanins CD9 and CD81. *Nat Commun* (2013) 4:1674. doi: 10.1038/ncomms2675.
23. Sala-Valdes M, Ursa A, Charrin S, Rubinstein E, Hemler ME, Sanchez-Madrid F, et al. EWI-2 and EWI-F link the tetraspanin web to the actin cytoskeleton through their direct association with ezrin-radixin-moesin proteins. *J Biol Chem* (2006) 281(28):19665-75. doi: 10.1074/jbc.M602116200.
24. Stipp CS, Kolesnikova TV, Hemler ME. EWI-2 is a major CD9 and CD81 partner and member of a novel Ig protein subfamily. *J Biol Chem* (2001) 276(44):40545-54. doi: 10.1074/jbc.M107338200.
25. Charrin S, Le Naour F, Labas V, Billard M, Le Caer JP, Emile JF, et al. EWI-2 is a new component of the tetraspanin web in hepatocytes and lymphoid cells. *Biochem J* (2003) 373(Pt 2):409-21. doi: 10.1042/bj20030343.
26. Rocha-Perugini V, Montpellier C, Delgrange D, Wychowski C, Helle F, Pillez A, et al. The CD81 partner EWI-2wint inhibits hepatitis C virus entry. *PLoS One* (2008) 3(4):e1866. doi: 10.1371/journal.pone.0001866.
27. Montpellier C, Tews BA, Poitrimole J, Rocha-Perugini V, D'Arienzo V, Potel J, et al. Interacting regions of CD81 and two of its partners, EWI-2 and EWI-2wint, and their effect on hepatitis C virus infection. *J Biol Chem* (2011) 286(16):13954-65. doi: 10.1074/jbc.M111.220103.
28. Gordon-Alonso M, Sala-Valdes M, Rocha-Perugini V, Perez-Hernandez D, Lopez-Martin S, Ursa A, et al. EWI-2 association with alpha-actinin regulates T cell immune synapses and HIV viral infection. *J Immunol* (2012) 189(2):689-700. doi: 10.4049/jimmunol.1103708.
29. Chen A, Leikina E, Melikov K, Podbilewicz B, Kozlov MM, Chernomordik LV. Fusion-pore expansion during syncytium formation is restricted by an actin network. *J Cell Sci* (2008) 121(Pt 21):3619-28. doi: 10.1242/jcs.032169.

30. Maddon PJ, Dalgleish AG, Mcdougal JS, Clapham PR, Weiss RA, Axel R. The T4 Gene Encodes the Aids Virus Receptor and Is Expressed in the Immune-System and the Brain. *Cell* (1986) 47(3):333-48. doi: 10.1016/0092-8674(86)90590-8.
31. Platt EJ, Wehrly K, Kuhmann SE, Chesebro B, Kabat D. Effects of CCR5 and CD4 cell surface concentrations on infections by macrophagetropic isolates of human immunodeficiency virus type 1. *J Virol* (1998) 72(4):2855-64.
32. Derdeyn CA, Decker JM, Sfakianos JN, Wu X, O'Brien WA, Ratner L, et al. Sensitivity of human immunodeficiency virus type 1 to the fusion inhibitor T-20 is modulated by coreceptor specificity defined by the V3 loop of gp120. *J Virol* (2000) 74(18):8358-67.
33. Wei X, Decker JM, Liu H, Zhang Z, Arani RB, Kilby JM, et al. Emergence of resistant human immunodeficiency virus type 1 in patients receiving fusion inhibitor (T-20) monotherapy. *Antimicrob Agents Chemother* (2002) 46(6):1896-905.
34. Takeuchi Y, McClure MO, Pizzato M. Identification of gammaretroviruses constitutively released from cell lines used for human immunodeficiency virus research. *J Virol* (2008) 82(24):12585-8. doi: 10.1128/jvi.01726-08.
35. Platt EJ, Bilska M, Kozak SL, Kabat D, Montefiori DC. Evidence that ecotropic murine leukemia virus contamination in TZM-bl cells does not affect the outcome of neutralizing antibody assays with human immunodeficiency virus type 1. *J Virol* (2009) 83(16):8289-92. doi: 10.1128/JVI.00709-09.
36. Nara PL, Hatch WC, Dunlop NM, Robey WG, Arthur LO, Gonda MA, et al. Simple, rapid, quantitative, syncytium-forming microassay for the detection of human immunodeficiency virus neutralizing antibody. *AIDS Res Hum Retroviruses* (1987) 3(3):283-302. doi: 10.1089/aid.1987.3.283.
37. Nara PL, Fischinger PJ. Quantitative infectivity assay for HIV-1 and-2. *Nature* (1988) 332(6163):469-70. doi: 10.1038/332469a0.
38. Refsland EW, Hultquist JF, Harris RS. Endogenous origins of HIV-1 G-to-A hypermutation and restriction in the nonpermissive T cell line CEM2n. *PLoS Pathog* (2012) 8(7):e1002800. doi: 10.1371/journal.ppat.1002800.
39. Simm M, Shahabuddin M, Chao W, Allan JS, Volsky DJ. Aberrant Gag protein composition of a human immunodeficiency virus type 1 vif mutant produced in primary lymphocytes. *J Virol* (1995) 69(7):4582-6.
40. Freed EO, Martin MA. Virion incorporation of envelope glycoproteins with long but not short cytoplasmic tails is blocked by specific, single amino acid substitutions in the human immunodeficiency virus type 1 matrix. *J Virol* (1995) 69(3):1984-9.
41. Krementsov DN, Weng J, Lambele M, Roy NH, Thali M. Tetraspanins regulate cell-to-cell transmission of HIV-1. *Retrovirology* (2009) 6:64. doi: 10.1186/1742-4690-6-64.
42. Karn J, Stoltzfus CM. Transcriptional and posttranscriptional regulation of HIV-1 gene expression. *Cold Spring Harb Perspect Med* (2012) 2(2):a006916. doi: 10.1101/cshperspect.a006916.
43. Sato K, Aoki J, Misawa N, Daikoku E, Sano K, Tanaka Y, et al. Modulation of human immunodeficiency virus type 1 infectivity through incorporation of tetraspanin proteins. *J Virol* (2008) 82(2):1021-33. doi: 10.1128/jvi.01044-07.
44. Nydegger S, Khurana S, Krementsov DN, Foti M, Thali M. Mapping of tetraspanin-enriched microdomains that can function as gateways for HIV-1. *J Cell Biol* (2006) 173(5):795-807. doi: 10.1083/jcb.200508165.

45. Jolly C, Sattentau QJ. Human immunodeficiency virus type 1 assembly, budding, and cell-cell spread in T cells take place in tetraspanin-enriched plasma membrane domains. *J Virol* (2007) 81(15):7873-84. doi: 10.1128/JVI.01845-06.
46. Krementsov DN, Rassam P, Margeat E, Roy NH, Schneider-Schaulies J, Milhiet PE, et al. HIV-1 assembly differentially alters dynamics and partitioning of tetraspanins and raft components. *Traffic* (2010) 11(11):1401-14.
47. Clark KL, Zeng Z, Langford AL, Bowen SM, Todd SC. PGRL is a major CD81-associated protein on lymphocytes and distinguishes a new family of cell surface proteins. *J Immunol* (2001) 167(9):5115-21.
48. Wang HX, Sharma C, Knoblich K, Granter SR, Hemler ME. EWI-2 negatively regulates TGF-beta signaling leading to altered melanoma growth and metastasis. *Cell Res* (2015) 25(3):370-85. doi: 10.1038/cr.2015.17.
49. Lambele M, Koppensteiner H, Symeonides M, Roy NH, Chan J, Schindler M, et al. Vpu is the main determinant for tetraspanin downregulation in HIV-1-infected cells. *J Virol* (2015) 89(6):3247-55. doi: 10.1128/jvi.03719-14.
50. Haller C, Muller B, Fritz JV, Lamas-Murua M, Stolp B, Pujol FM, et al. HIV-1 Nef and Vpu are functionally redundant broad-spectrum modulators of cell surface receptors, including tetraspanins. *J Virol* (2014) 88(24):14241-57. doi: 10.1128/jvi.02333-14.
51. Greenwood EJ, Matheson NJ, Wals K, van den Boomen DJ, Antrobus R, Williamson JC, et al. Temporal proteomic analysis of HIV infection reveals remodelling of the host phosphoproteome by lentiviral Vif variants. *Elife* (2016) 5. doi: 10.7554/eLife.18296.
52. Naamati A, Williamson JC, Greenwood EJ, Marelli S, Lehner PJ, Matheson NJ. Functional proteomic atlas of HIV-infection in primary human CD4+ T cells. *bioRxiv* (2018). doi: 10.1101/389346.
53. Ikeda T, Symeonides M, Albin JS, Li M, Thali M, Harris RS. HIV-1 adaptation studies reveal a novel Env-mediated homeostasis mechanism for evading lethal hypermutation by APOBEC3G. *PLoS Pathog* (2018) 14(4):e1007010. doi: 10.1371/journal.ppat.1007010.
54. Chuprin A, Gal H, Biron-Shental T, Biran A, Amiel A, Rozenblatt S, et al. Cell fusion induced by ERVWE1 or measles virus causes cellular senescence. *Genes Dev* (2013) 27(21):2356-66. doi: 10.1101/gad.227512.113.

Figure Legends

Figure 1. EWI-2 co-accumulates with Gag at the HIV-1 VS in T cells

(A) CEM-SS cells infected with HIV-1 NL4-3 WT or ΔEnv were co cultured with either CMAC-labeled CEM-SS (blue) or unlabeled TZM-bl target cells (which have much lower basal EWI-2 surface levels) for 5 h, and subsequently stained for surface EWI-2 (red) and Gag (green). Enrichment of EWI-2 was calculated by measuring the EWI-2-associated fluorescence intensity at cell-cell contact sites and dividing that by the sum of the average non-contact site fluorescence of both producer and target cells (graphed data represent a quantification of the experiment with CEM-SS target cells). (B) Primary $CD4^+$ T cells infected with HIV-1 NL4-3 were co-cultured with uninfected target primary cells for 2 h and stained for EWI-2 (red) and Gag (green). Enrichment of EWI-2 at Env-dependent (WT) or Env-independent (ΔEnv) infected-uninfected cell contacts was quantified as described in (A). Scale bars = 10 µm. *p*-values are the result of two-tailed non-parametric Mann-Whitney *U* tests.

Figure 2. EWI-2 is downregulated from the surface of infected cells.

(A) CEM2n cells were infected with NL-sfGI and surface-labeled for EWI-2, fixed, stained with DAPI (shown in blue) and Alexa Fluor 594-conjugated secondary antibody, and imaged. GFP signal (green) was used to identify infected cells, and EWI-2-associated signal is shown pseudocolored in red. Representative cells are shown. Scale bars = 10 µm. (B) Cells were prepared as in (A) and scored as EWI-2 WT or EWI-2 low. Bars represent the mean percentage of uninfected and infected cells scored as EWI-2 WT from 3 separate experiments. Error bars = standard deviation of the mean (SD). (C) CEM2n cells were infected with NL-sfGI and surface-labeled for EWI-2, fixed, and stained with Alexa Fluor 647-conjugated secondary antibody, and analyzed by flow cytometry. Left; Bars represent the average percentage of uninfected and infected cells (within the same tube) that were EWI-2 WT from 3 separate experiments. Error bars = SD. Right; EWI-2 surface expression was measured by mean fluorescence intensity (MFI) of EWI-2-associated signal. Lines connect paired data points, i.e. infected cells and uninfected cells (within an infected tube) from the same biological replicate. (D) Primary CD4+ T cells were infected, plated, and surface-labeled for EWI-2 as described in (A). EWI-2 levels at the plasma membrane in infected and uninfected cells were measured by manually selecting the plasma membrane at the midline of each cell and quantifying the mean EWI-2-associated fluorescence intensity. Data shown are pooled from two biological replicates, each consisting of two technical replicates. Only cells which were not in contact with other cells were quantified. *p*-values are the result of student's paired *t*-tests (B-C) or a two-tailed non-parametric Mann-Whitney *U* test (D).

Figure 3. EWI-2 overexpression represses infected-uninfected cell fusion.

(A) HeLa-TZM-bl fusion assays were performed using producer HeLa cells that were co-transfected with either pNL-sfGI ΔEnv (ΔEnv) or pNL-sfGI (WT) in combination with either EWI-2 (blue), CD81 (red), or L6 overexpression plasmids. Luminescence readings (across 5 independent biological replicates, each with 2 technical replicates) were divided by the ΔEnv condition to obtain the fold increase in fusion, and then normalized to the WT co-transfected with L6 condition (represented by the dashed line). Error bars = SD. (B) Fusion assays were performed as described above using producer HeLa cells co-transfected with WT alongside EWI-2 and CD81, or EWI-2 and CD81 independently. All samples (across 2 independent biological replicates, each with 3 technical replicates) were normalized to ΔEnv and then to WT/L6 as above, and values were expressed as a percentage reduction of fusion from WT/L6 (i.e. higher values indicate less fusion). Error bars = SD.

A

CEM-SS cells

Virus

Targets

Gag | EWI-2 | Merge

CEM-SS — WT

CEM-SS — ΔEnv

TZM-bl — WT

TZM-bl — ΔEnv

10 µm

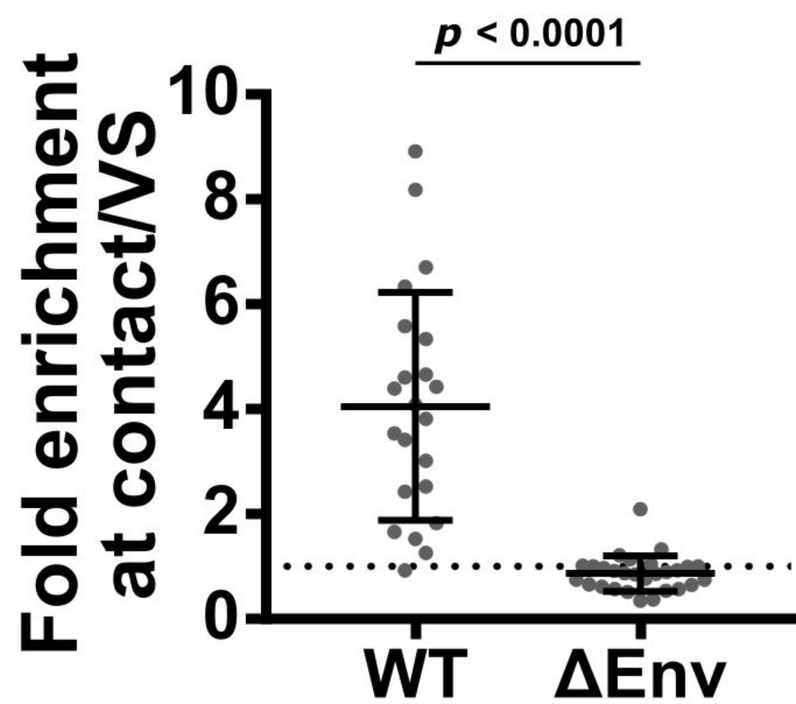

B

Primary CD4+ T cells

Gag | EWI-2 | Merge

WT

ΔEnv

10 µm

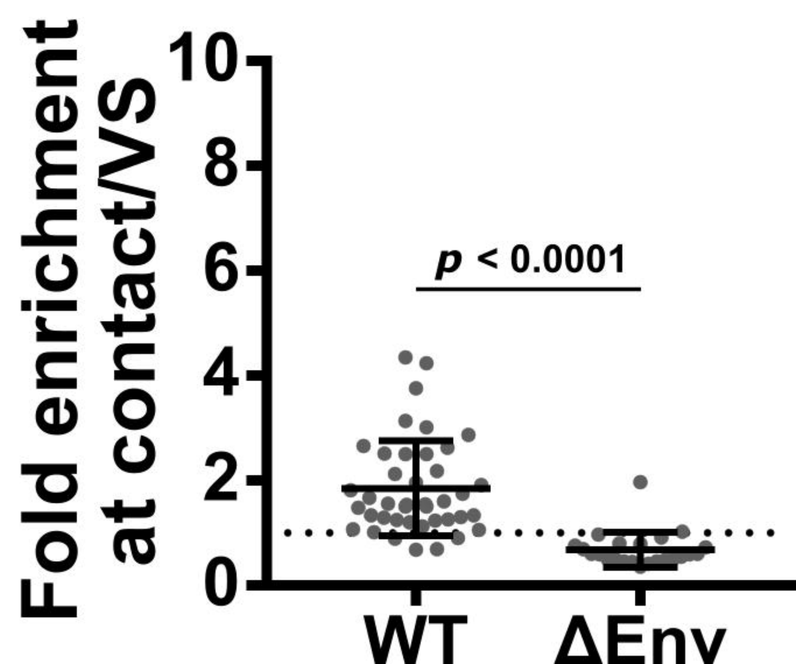

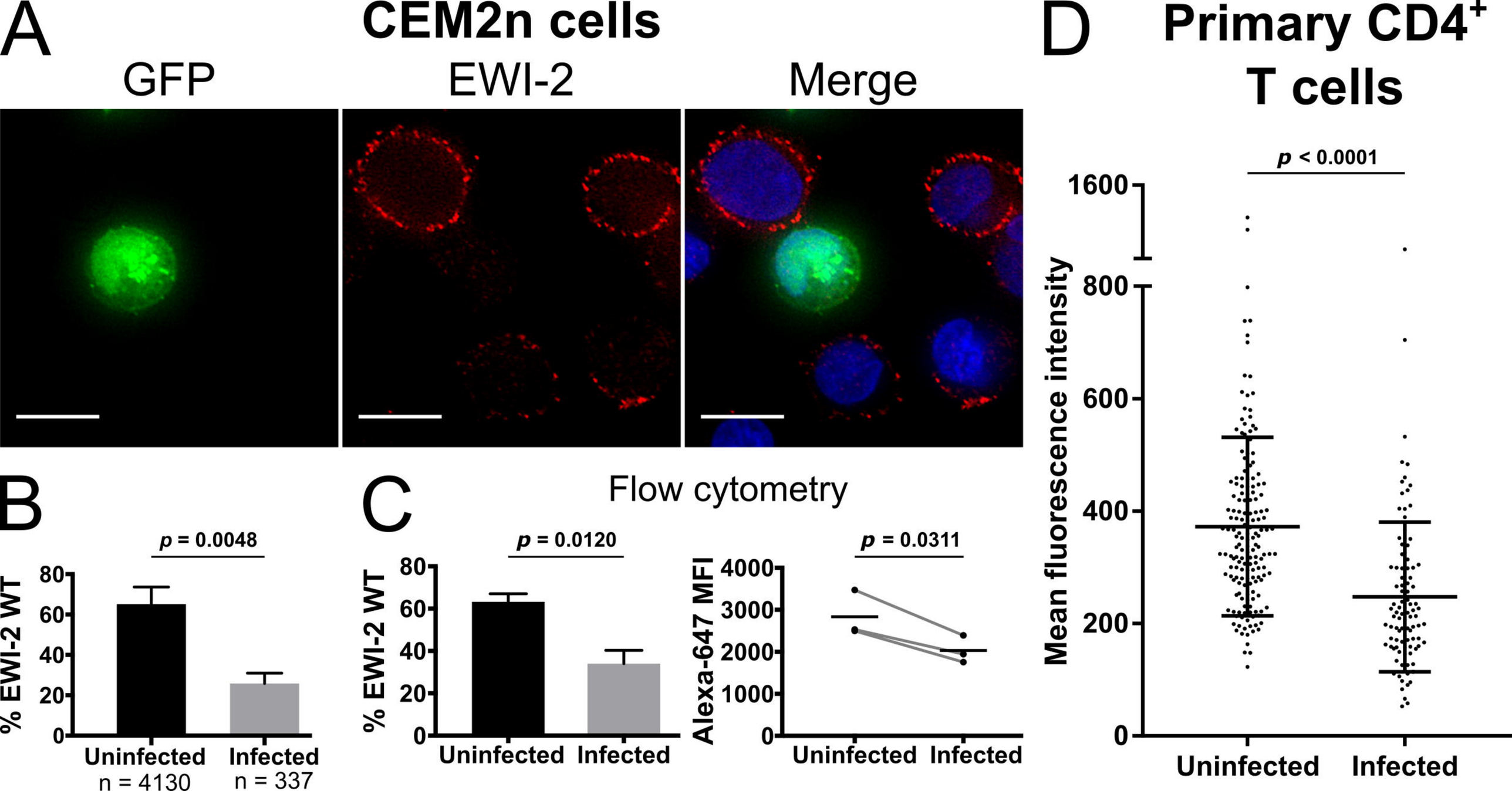
A
CEM2n cells
GFP
EWI-2
Merge
B
p = 0.0048
% EWI-2 WT
80
60
40
20
0
Uninfected
n = 4130
Infected
n = 337
C
Flow cytometry
p = 0.0120
% EWI-2 WT
80
60
40
20
0
Uninfected
Infected
p = 0.0311
Alexa-647 MFI
4000
3000
2000
1000
0
Uninfected
Infected
D
Primary CD4+
T cells
p < 0.0001
Mean fluorescence intensity
1600
800
600
400
200
0
Uninfected
Infected

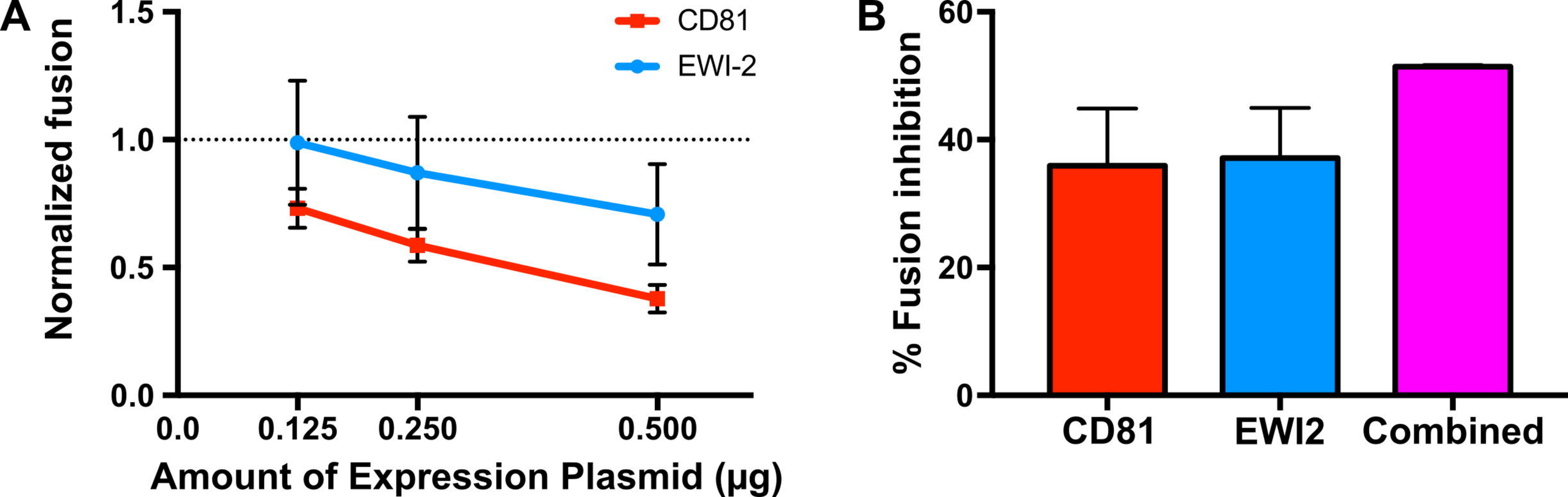
A
Normalized fusion
1.5
1.0
0.5
0.0
CD81
EWI-2
0.0
0.125
0.250
0.500
Amount of Expression Plasmid (µg)
B
% Fusion inhibition
60
40
20
0
CD81
EWI2
Combined